

Lambda transverse polarization in NA61/SHINE at the CERN SPS: feasibility studies

YEHOR BONDAR

Institute of Physics, Jan Kochanowski University, 25-406 Kielce, Poland

WOJCIECH FLORKOWSKI

Institute of Theoretical Physics, Jagiellonian University, 30-348 Kraków, Poland

Received August 21, 2024

The spin polarization of Λ hyperons produced in inclusive reactions with unpolarized protons on unpolarized targets has been studied for almost 40 years. The NA61/SHINE experiment at the CERN SPS has a great potential to study transverse polarization in p-p and p-A collisions. In this work, we discuss the impact of magnetic field and limited detector acceptance on the possible polarization measurement by this experiment. Our analysis shows that the magnetic field impact on the Λ polarization due to precession is one order of magnitude smaller than the detector acceptance-based polarization bias, and the identification of an experimental signal similar to that observed before by other experiments is possible.

1. Introduction

The spin polarization of Λ hyperons produced in inclusive reactions with unpolarized protons on unpolarized targets has been already studied over a wide range of reaction energies and various production angles of the Λ hyperons [1–8]. Several theoretical models have been proposed to describe experimental data [9–11], however, the mechanism of polarization is still not well understood. In this work, we analyze the impact of magnetic field and limited detector acceptance on the possible polarization measurement by the NA61/SHINE experiment [12] at the CERN SPS.

NA61/SHINE uses two super-conducting magnets. The standard current setting for data taking at the beam momentum of 158 GeV/c corresponds to the full field of 1.5 T in the first magnet and the reduced field of 1.1 T in the second magnet, with a maximum total bending power up to 9 Tm. Magnetic field magnitude along beamline is shown in Fig. 1.

The NA61/SHINE Collaboration already published the results on Λ production in p+p interactions at the beam momentum of 158 GeV/c [13].

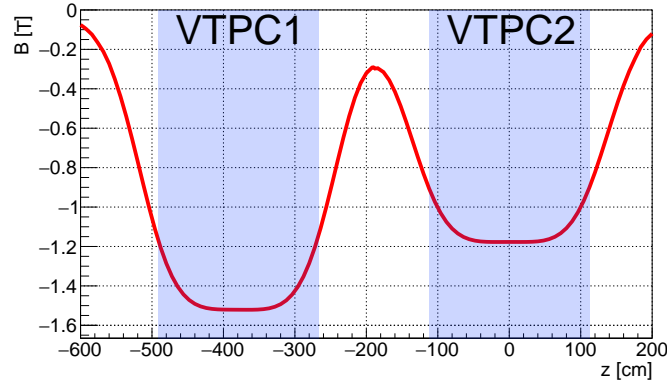


Fig. 1. Magnetic field along the beamline (z) direction in the NA61/SHINE reference frame. Here $x = y = 0$ and the field has only the (negative) y -component.

About 50 million proton-proton collision events were recorded in the years 2009–2011, providing an opportunity to measure Λ transverse polarization at the previously unstudied center-of-mass energy $\sqrt{s} = 17.3$ GeV. The NA61/SHINE spectrometer has coverage of Λ in the range of transverse momentum $p_T \in (0, 1.6)$ GeV/ c and the Feynman variable $|x_F| \lesssim 0.4$ [13], which is the region with maximal magnitude of the expected polarization.

To study the properties of Λ hyperons, in this work $1.2 \cdot 10^8$ events of p+p inelastic collisions with 158 GeV/ c beam momentum were generated by the Epos1.99 model (version CRMC 1.4) [14, 15], and subsequently passed through a detector simulation employing the Geant3 package [16]. Simulated p+p interactions are placed uniformly at $z \in [-590, -570]$ cm and 3 cm in diameter around $(x, y) = (0, 0)$ to reproduce a 20 cm long (2.8 % of nuclear interaction length) liquid hydrogen target (LHT) position in NA61/SHINE detector setup. As a result, $8.7 \cdot 10^6$ Λ s with $p\pi^-$ decay channel were analyzed.

Hereinafter the LAB frame denotes the NA61/SHINE frame, while the rest frame refers to the Λ rest frame. Natural units $\hbar = c = 1$ are commonly used, except for several places where c is explicitly displayed.

2. Transverse polarization – effects of cuts

The production plane coordinate system is defined by three mutually orthogonal unit vectors: \hat{n}_z directed along Λ momentum, \hat{n}_x is transverse

to beam and Λ momenta, \hat{n}_y forms right-handed system,

$$\hat{n}_x = \frac{\vec{p}_{\text{beam}} \times \vec{p}_\Lambda}{|\vec{p}_{\text{beam}} \times \vec{p}_\Lambda|}, \quad \hat{n}_z = \frac{\vec{p}_\Lambda}{|\vec{p}_\Lambda|}, \quad \hat{n}_y = \hat{n}_z \times \hat{n}_x, \quad (1)$$

where \vec{p}_Λ is the Λ momentum in LAB, and \vec{p}_{beam} is the incident proton beam momentum. In order to obtain transverse polarization, the following steps are required:

- rotation from LAB to the production plane coordinate system (1),
- boost along \hat{n}_z to the Λ rest frame, with the Lorentz transformation parameters $\beta = |\vec{p}_\Lambda|/E_\Lambda$ and $\gamma = (1 - \beta^2)^{-1/2} = E_\Lambda/m_\Lambda$, where E_Λ is the Λ total energy in LAB and $m_\Lambda = 1.115 \text{ GeV}/c^2$ is the Λ mass [17],
- calculation of the cosines of the angles between the vector \vec{p}_p^* and the directions of the three axes,

$$\cos \theta_i = \frac{p_{pi}^*}{|\vec{p}_p^*|}, \quad i = x, y, z, \quad (2)$$

- fitting the $\cos \theta_i$ distributions and extraction of the polarization vectors P_i , using a theoretically predicted distribution of proton momentum direction $f(\cos \theta_i)$

$$f(\cos \theta_i) = \frac{1 + \alpha P_i \cos \theta_i}{2}, \quad (3)$$

where $\alpha = 0.732 \pm 0.014$ is the asymmetry parameter of the parity-violating weak decay of the Λ hyperon [17].

For simulations with unpolarized protons and without any microscopic mechanism for the spin Λ polarization (the case of Epos), one expects that $f(\cos \theta_i) = 0.5$. However, due to a finite detector coverage in space not all Λ decays can be recorded and this introduces a bias. To include the NA61/SHINE geometry in our analysis, the following selection Λ track cuts were imposed:

- number of hits in VTPC's ≥ 15 for both proton and pion tracks¹,

¹ During the reconstruction procedure, some minimum amount of the tracks' hits are required for good momentum resolution.

- for the difference between the z coordinate of Λ vertex (decay point) and the primary vertex, $\Delta z = z_\Lambda - z_{PV}$, a rapidity² dependent cut was applied: $\Delta z > 10$ cm for $y < 0.25$, $\Delta z > 15$ cm for $0.25 \leq y \leq 0.75$, $\Delta z > 40$ cm for $0.75 \leq y \leq 1.25$, and $\Delta z > 60$ cm for $y > 1.25$.

We note that these cuts are analogous to the cuts used in Ref. [13].

The angular proton distributions resulting from the application of the cuts defined above to initially uniform distributions are shown in Fig. 2. The largest deviations from 0.5 are seen for P_z .

3. Lambda precession in a magnetic field (classical treatment)

As the Λ hyperon has a nonzero magnetic moment, it does interact with the magnetic field inside the Time Projection Chambers. Consequently, one has to investigate and quantitatively estimate whether a magnetic field can influence the polarization measurements (in addition to the cuts studied earlier).

The classical covariant equation describing the spin motion, known as the Bargmann–Michel–Telegdi (BMT) equation, has the following form [18]

$$\frac{dS^\alpha}{d\tau} = \frac{ge}{2m} \left[F^{\alpha\beta} S_\beta + u^\alpha \left(S_\lambda F^{\lambda\mu} u_\mu \right) \right] - u^\alpha \left(S_\lambda \frac{du^\lambda}{d\tau} \right), \quad (4)$$

where S^α is the Pauli-Lubański spin 4-vector, u^α is the 4-velocity of a particle, and τ is the proper time. Here $\frac{ge}{2m} = \mu_\Lambda \mu_N$, where μ_N is the nuclear magneton and $\mu_\Lambda = -0.613$ is the magnetic moment of Λ in μ_N units [17]. As gradient force terms like $\nabla(\vec{m} \cdot \vec{B})$ are negligible (see Appendix) and there are no other forces due to the fact that Λ is a neutral particle, the last term in Eq. (4) can be ignored. Hence, in the Λ rest frame the spin evolution is described by the formula

$$\frac{d\vec{S}}{d\tau} = \mu_\Lambda \mu_N \left[\vec{S} \times \vec{B}' \right], \quad (5)$$

where \vec{B}' is the magnetic field in rest frame in terms of the NA61/SHINE magnetic field \vec{B} (electric field in LAB has been neglected³)

$$\vec{B}' = \gamma \vec{B} - (\gamma - 1)(\vec{B} \cdot \vec{p}_\Lambda) \vec{p}_\Lambda / |\vec{p}_\Lambda|^2. \quad (6)$$

² The rapidity is defined in the standard way as $y = \tanh^{-1}(p_L/E)$, where p_L and E are longitudinal momentum and energy of the Λ in the center-of-mass frame.

³ Electric field in TPC is $E = 195$ V/cm, which gives $E/(cB) \approx 4 \cdot 10^{-5}$.

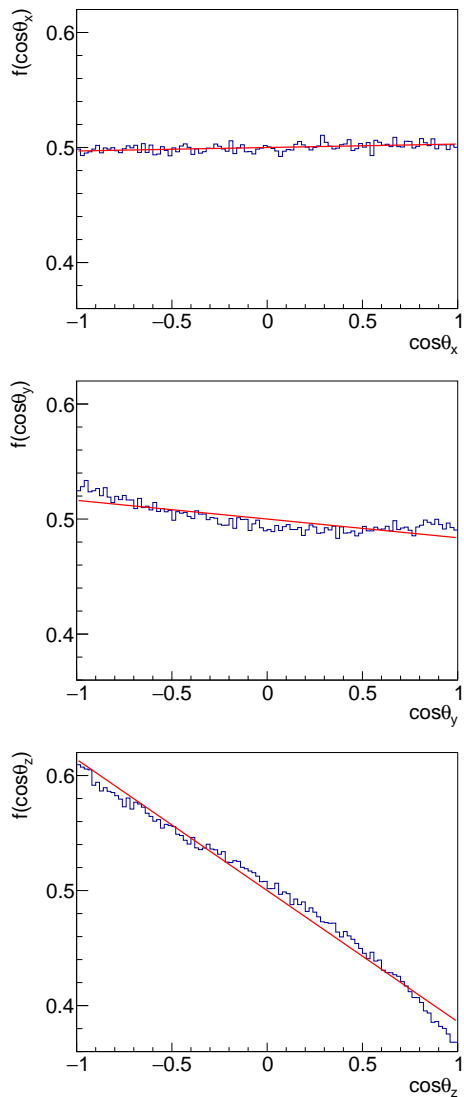


Fig. 2. Angular distributions after application of the cuts specified in the text. Fitting to the function (3) gives $P_x = -0.01$, $P_y = -0.04$, and $P_z = -0.31$.

To compute the angle of precession, we numerically integrate Eq. (5). The spatial dependence of the magnetic field strength $\vec{B}(\vec{r})$ is taken from the NA61/SHINE software package. For further convenience, we consider

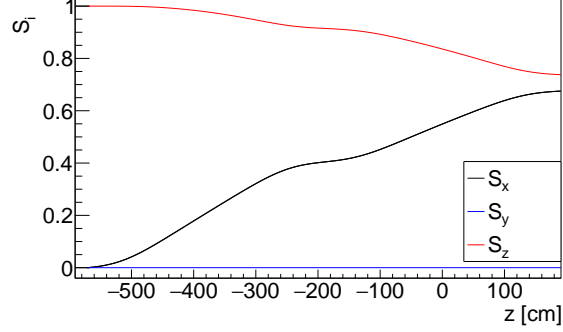


Fig. 3. An extreme example showing the evolution of the spin vector components of the Λ hyperon in the NA61/SHINE spectrometer magnetic field for the momentum $\vec{p}_\Lambda = (0, 0, 40)$ GeV/c.

the change of variables to $dz = \frac{v_z}{m} cd\tau$ and rewrite Eq. (5) as

$$\frac{d\vec{S}}{dz} = \frac{\mu_\Lambda \mu_N}{(p_z/m)} \left[\vec{S} \times \vec{B}'(\vec{r}) \right]. \quad (7)$$

Finally, the integration over the z coordinate with step $\Delta z = 1$ cm is made.

An example of the space evolution of the three spin vector components of Λ in the NA61/SHINE spectrometer magnetic field for the momentum $\vec{p}_\Lambda = (0, 0, 40)$ GeV/c is shown in Fig. 3. In this case the distance travelled by Λ is quite substantial due to the time dilation effect caused by the large Λ momentum.

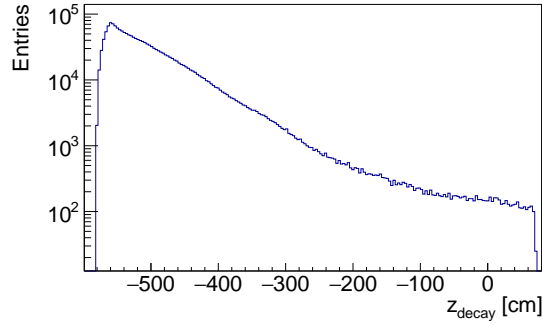


Fig. 4. The distribution of the coordinates z_{decay} (after cuts).

The largest value of z_{decay} shown in Fig. 3 is possible only for most energetic Λ s, however, taking into account the exponential law of decay, the

majority of particles simulated with Epos decays with $z_{\text{decay}} < -400$ cm, which is shown in Fig. 4. Dependence of the corresponding precession angle ϕ_{max} on position of decay z_{decay} is shown in Fig. 5. It may reach 0.35, however, for most of the particles, it remains below 0.1.

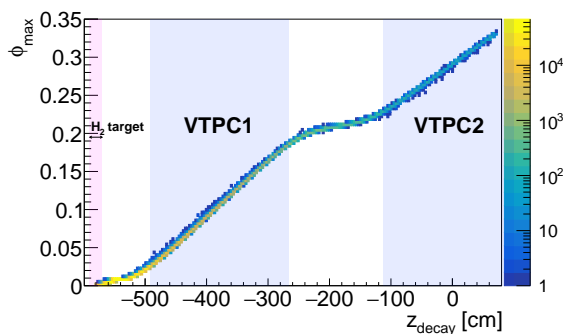


Fig. 5. Dependence of the maximum precession angle ϕ_{max} on the z coordinate point of Λ decay z_{decay} .

The same numerical simulations can be used to determine the influence of the magnetic field on the polarization measurement bias. The initial Λ polarization vector \vec{S} was generated uniformly in space and propagated in the magnetic field until the particle's decay, according to Eq. (7). Next, the vector \vec{S} projected along the directions \hat{n}_x , \hat{n}_y , and \hat{n}_z . The distributions of the polarization vector components before and after the evolutions are presented in Figs. 6 and 7. The polarization bias components defined as $P_i = \langle S_i \rangle$ are shown in Fig. 8. We see an effect smaller than 10^{-2} , consistent with zero for many of (x_F, p_T) bins.

4. Summary

Our main conclusions can be summarized by two points: first, the geometrical acceptance significantly biases the polarization results and should be taken into account via MC corrections, second, the impact of the magnetic field on Λ polarization due to precession is at least one order of magnitude smaller than detector acceptance-based polarization bias.

Consequently, we expect that NA61/SHINE has a large potential to study Λ transverse polarization in p-p collisions. The identification of an experimental signal similar to that observed before by other experiments is possible (see, for example, Refs. [3–5, 7, 8]).

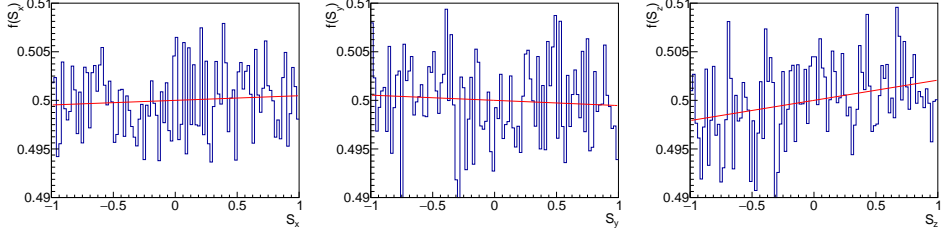


Fig. 6. Polarization vector \vec{S}_{init} distribution. Fitted values are $P_x = (1.3 \pm 1.8) \cdot 10^{-3}$, $P_y = (-1.5 \pm 1.8) \cdot 10^{-3}$, and $P_z = (5.7 \pm 1.8) \cdot 10^{-3}$.

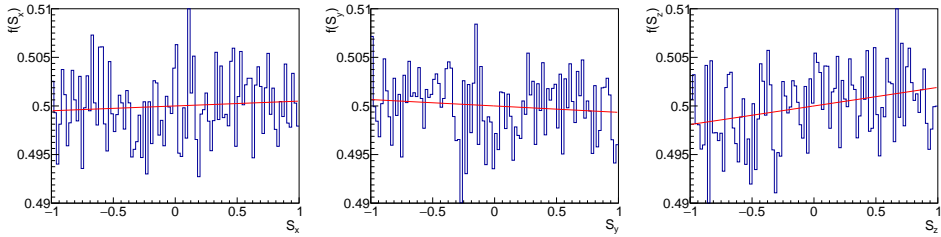


Fig. 7. Polarization vector \vec{S} distribution. Fitted values are $P_x = (1.4 \pm 1.8) \cdot 10^{-3}$, $P_y = (-1.8 \pm 1.8) \cdot 10^{-3}$, and $P_z = (5.2 \pm 1.8) \cdot 10^{-3}$.

Acknowledgements

Y.B. is grateful to the NA61/SHINE collaboration for providing the Monte-Carlo data and computational facilities and M. Gaździcki for fruitful discussions. This work was supported in part by the Polish National Science Centre Grant No. 2022/47/B/ST2/01372 (WF) and 2023/49/N/ST2/02299 (YB).

5. Appendix: gradient force

Here we make an estimate of the impact of the force $\vec{F} = \vec{\nabla}(\vec{m} \cdot \vec{B}) = \sum_k m_k \vec{\nabla} B_k$ (for $k = x, y, z$, where \vec{m} is particle's magnetic moment) on the polarization evolution. In the laboratory frame, the magnetic field changes by $\Delta B_y \simeq 1.5$ T over the distance $L \simeq 1.5$ m along z -axis. Due to time dilation, the particle flight path is $L = \gamma c\tau$, where τ is the Λ mean lifetime and $c\tau = 7.89$ cm. Hence, $\gamma \simeq 19$ and the hyperon momentum $p_\Lambda \simeq 21$ GeV/ c , which is a typical Λ momentum for proton-proton collisions at 158 GeV/ c beam momentum. Numerical value of nuclear magneton is $\mu_N = 3 \cdot 10^{-8}$ eV/T, and the Λ magnetic moment $|\vec{m}| \approx 0.6\mu_N$. In the Λ rest frame, the momentum change is $\Delta\vec{p} = \vec{F}\tau = m_y \vec{\nabla} B_y \tau$. Even if \vec{m} is aligned

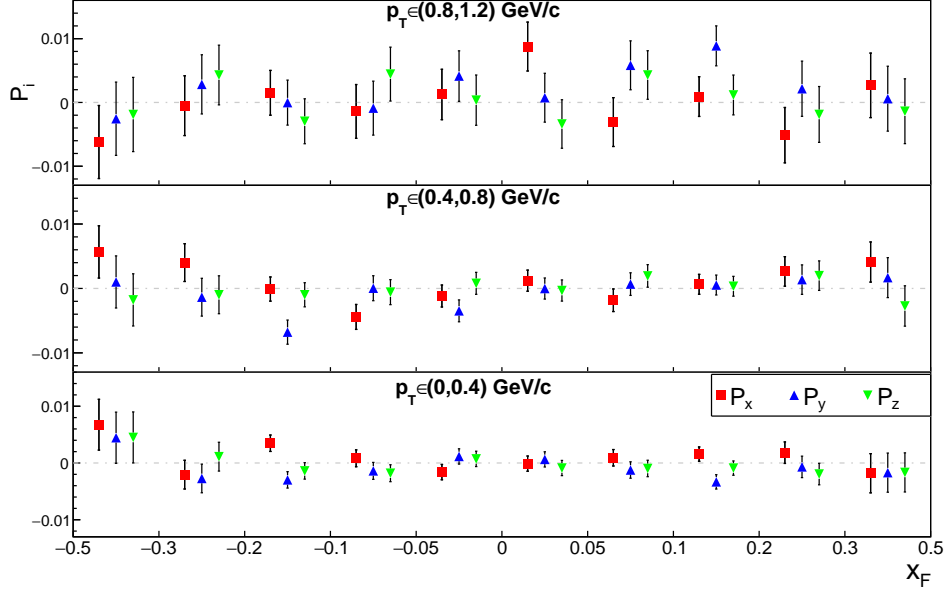


Fig. 8. Polarization vector P_i distribution for different (x_F, p_T) binning.

with the y -axis, we find

$$\Delta p_z = 0.6\mu_N \frac{\gamma \Delta B_y}{L/\gamma} \tau \approx 5 \cdot 10^{-7} \text{ eV}/c. \quad (8)$$

Therefore, $v/c = p_z/(mc) \approx 5 \cdot 10^{-16}$ and this ratio is negligible. From the BMT equation (4), the spin vector change is quadratic in the speed of particle: $|\Delta \vec{S}| \sim (v/c)^2 \sim 10^{-31}$, hence, the impact of the gradient force can be neglected.

REFERENCES

- [1] S. Erhan et al. Λ^0 polarization in proton-proton interactions at $\sqrt{s} = 53$ GeV and 62 GeV. *Physics Letters B*, 82(2):301–304, 1979.
- [2] G. Bunce et al. Λ^0 hyperon polarization in inclusive production by 300-GeV protons on beryllium. *Phys. Rev. Lett.*, 36:1113–1116, May 1976.
- [3] G. Aad et al. Measurement of the transverse polarization of Λ and $\bar{\Lambda}$ hyperons produced in proton-proton collisions at $\sqrt{s} = 7$ TeV using the atlas detector. *Phys. Rev. D*, 91:032004, Feb 2015.

- [4] I. Abt et al. Polarization of Λ and $\bar{\Lambda}$ in 920 GeV fixed-target proton–nucleus collisions. *Phys. Lett. B*, 638(5):415–421, 2006.
- [5] V. Fanti et al. A measurement of the transverse polarization of Λ -hyperons produced in inelastic pn-reactions at 450 GeV proton energy. *The European Physical Journal C*, 6(2):265–269, Jan 1999.
- [6] E. J. Ramberg et al. Polarization of Λ and $\bar{\Lambda}$ produced by 800-GeV protons. *Phys. Lett. B*, 338(2):403–408, 1994.
- [7] B. Lundberg et al. Polarization in inclusive Λ and $\bar{\Lambda}$ production at large p_T . *Phys. Rev. D*, 40:3557–3567, Dec 1989.
- [8] A. D. Panagiotou. Λ^0 polarization in hadron-nucleon, hadron-nucleus and nucleus-nucleus interactions. *International Journal of Modern Physics A*, 05(07):1197–1266, 1990.
- [9] Bo Andersson, G. Gustafson, and G. Ingelman. A semiclassical model for the polarization on inclusively produced Λ^0 -particles at high energies. *Physics Letters B*, 85(4):417–420, 1979.
- [10] J. Szwed. Hyperon polarization at high energies. *Physics Letters B*, 105(5):403–405, 1981.
- [11] T. A. DeGrand and H. I. Miettinen. Models for polarization asymmetry in inclusive hadron production. *Phys. Rev. D*, 24:2419–2427, Nov 1981.
- [12] N. Abgrall et al. NA61/SHINE facility at the CERN SPS: beams and detector system. *JINST*, 9:P06005, 2014.
- [13] A. Aduszkiewicz et al. Production of Λ -hyperons in inelastic p+p interactions at 158 GeV/c. *The European Physical Journal C*, 76(198), 2016.
- [14] K. Werner, F.-M. Liu, and T. Pierog. Parton ladder splitting and the rapidity dependence of transverse momentum spectra in deuteron-gold collisions at RHIC. *Phys. Rev. C*, 74:044902, 2006.
- [15] T. Pierog and K. Werner. EPOS Model and Ultra High Energy Cosmic Rays. *Nucl. Phys. Proc. Suppl.*, 196:102–105, 2009.
- [16] René Brun et al. *GEANT: Detector Description and Simulation Tool; Oct 1994*. CERN Program Library. CERN, Geneva, 1993.
- [17] S. Navas et al. Review of particle physics. *Phys. Rev. D*, 110:030001, Aug 2024.
- [18] J. D. Jackson. *Classical Electrodynamics*. Wiley, 3 edition, 1999.